Energy Conversion and Management 86 (2014) 154–164

Contents lists available at ScienceDirect

Energy Conversion and Management

journal homepage: www.elsevier.com/locate/enconman

Analysis of thermal degradation kinetics and carbon structure changes of co-pyrolysis between macadamia nut shell and PET using thermogravimetric analysis and ^{13}C solid state nuclear magnetic resonance

Kwang-Hyun Ko [a], Aditya Rawal [b], Veena Sahajwalla [a,*]

[a] Centre for Sustainable Materials Research & Technology (SMaRT), School of Materials Science and Engineering, University of New South Wales, Sydney, NSW 2052, Australia
[b] Nuclear Magnetic Resonance Facility, Mark Wainwright Analytical Centre, University of New South Wales, Sydney, NSW 2052, Australia

ARTICLE INFO

Article history:
Received 19 August 2013
Accepted 20 April 2014
Available online 24 May 2014

Keywords:
Co-pyrolysis
Synergistic effect
Cross-linking of carbon structure
Thermogravimetric analysis (TGA)
Nuclear magnetic resonance (NMR)
Thermal degradation kinetics

ABSTRACT

Thermal degradation kinetics of co-pyrolysis of polyethylene terephthalate (PET) blended with macadamia nut shell were investigated using a large-scale customised thermogravimetric analysis (TGA) and ^{13}C solid-state nuclear magnetic resonance (NMR) spectroscopy. Blending ratios ranging 20–80 wt.% of PET with macadamia nut shell were analysed at heating rates of 3, 5 and 8 °C/min up to 1273 K in the presence of N_2 atmosphere with a flow rate of 1 L/min. The differential thermogravimetric analysis (DTG) data was analysed by the Freeman–Carroll method to yield kinetic parameters which were correlated with chemical analysis by ^{13}C solid-state NMR. The results indicated that two synergistic effects occurred between PET and macadamia nut shell during co-pyrolysis, which were characterised by an enhanced carbon yield of the co-pyrolysis products. The secondary reaction occurring between primary products of macadamia nut shell and PET was identified as the cause of the synergistic effect and this effect varied with weight fraction of macadamia nut shell in the blend and the heating rate. The measured changes in activation energy and reaction order indicated that the thermal degradation mechanism of co-pyrolysis is different to that of the individual components. The NMR results indicated that macadamia nut shell catalysed the degradation behaviour of PET leading to growth of polycyclic aromatic hydrocarbons (PAHs) through cross-linking reaction and enhancing the carbon yield from the PET.

1. Introduction

The co-pyrolysis of fossil fuel derived polymers with biomass in an inert atmosphere presents an alternative route to recycle waste polymers while implementing carbon capture of the renewable biomass. Intensive farming of crops such as macadamia can produce large quantities of waste biomass (exceeding 40,000 tonnes annually for the macadamia crop) [1]. Similarly nearly 15 million tonnes annually, of polymers such as polyethylene terephthalate (PET) are produced, primarily for the manufacture of disposable plastic drink bottles [2]. Instead of disposal in landfills or being used as an energy source in thermal power generation, co-pyrolysis technology enables the conversion of waste plastics and biomass into high value chemical feedstock that can replace dependence on fossil fuel [3,4]. The thermal treatment of plastics and biomass yields two fractions. The volatile light liquid fraction, known as tar can be downstream processed into various chemical feed stock. The condensed, high molecular weight fraction know as char, which is almost pure carbon has a variety of applications such as the carbon anode in aluminium production and graphite anode in lithium ion batteries [5,6]. Indeed the carbon derived from the pyrolysis of biomass and polymers at 1000 °C has outstanding electrochemical properties, comparable to those of graphite in some cases [7,8]. As a result, biomass and polymers have the potential to become an important alternative to replace petroleum coke as the carbon source for such applications.

The thermal degradation behaviour of synthetic polymers is relatively simple, even though the product yields from distinct polymers can be very different. For example, although both PET and polyolefins have single step primary degradation behaviour, the char yield of the PET pyrolysis is ca. ten times higher than that of polyolefins [9]. In comparison to synthetic polymers, biomass is predominantly a mix of three biopolymer components viz. cellulose, hemicellulose, and lignin. As expected from its multi-component nature, the thermal degradation of biomass is quite complex.

* Corresponding author.
E-mail address: veena@unsw.edu.au (V. Sahajwalla).

http://dx.doi.org/10.1016/j.enconman.2014.04.060
0196-8904/

TGA of macadamia nut shell in an inert atmosphere shows two main degradation regions from 565 K to 1075 K corresponding to the thermal degradation of hemicellulose and cellulose respectively [10]. Thermal degradation of lignin overlaps with that of both hemicellulose and cellulose. When biomass is heat treated in an inert atmosphere, the main components produce primary tar (primarily from the cellulose and hemicellulose) as well as primary char (from the lignin) over temperatures up to 820 K [11–13]. The primary char acts as a catalyst in converting the organic vapour to light gases by cracking reactions and then to secondary char by polymerisation reaction. The formation of char contributes to developing PAHs particularly during the low temperature (<800 K) stage of pyrolysis [12–16].

Co-pyrolysis of synthetic polymers with biomass enables the control of product distribution by varying the type and blend ratio of the raw materials. For example, previous studies on the co-pyrolysis of biomass and polyolefinic polymers have shown that the presence of biomass has a catalytic effect on the tar formation resulting in enhanced weight loss. The key factor for the enhanced weight loss is the hydrogen transfer from the degraded polyolefin (which have ca. 14 wt.% hydrogen) into the char-radical species (of the biomass) which prevents cross linking reactions to the char and thereby enhances the tar formation within the polyolefin [4,17–19]. On other hand polymers such as PET, which have a comparatively smaller weight fraction of hydrogen (4 wt.%), and produce high molecular weight aromatic products, may behave very differently in the presence of biomass during pyrolysis [9].

In the present work, we investigate the specific case of co-pyrolysis of macadamia nut shell biomass with PET to elucidate the co-pyrolysis kinetics and chemical structure which is at present poorly understood. We expect that due to its aromatic nature, PET has a distinct interaction with the biomass during co-pyrolysis which can enhance the end yield of the char residue.

The thermogravimetric analysis (TGA) is used to determine the overall thermal degradation kinetics which includes information such as the frequency factor, the activation energy and the overall reaction order [20]. Complementary to the TGA, ^{13}C solid-state nuclear magnetic resonance (NMR) spectroscopy yields specific information regarding the chemical structure of the solid pyrolysis product at the relevant pyrolysis temperatures [21]. The resulting insights allow the significantly different kinetic mechanisms of PET-biomass co-pyrolysis to be determined along with a molecular level characterisation of the co-degradation process. This study of the carbonisation process of these materials in the manner of single and co-pyrolysis is expected to significantly contribute to understanding of char properties including electrochemical applications and the developing efficient char utilisation technologies [21,22].

2. Experimental

2.1. Raw materials

The materials used in this study were macadamia nut shell in the powder form and commercial available PET pellets. The macadamia collected in Queensland, Australia was milled the particle size ranging from 0.25 mm to 2 mm. The milled macadamia nut shell was dried in air at 60 °C for at least 48 h. The commercial PET did not contain any fibres or filler.

2.2. Weight reduction measurement in non-isothermal thermogravimetric analysis (TGA)

A customised large scale TGA was used to study thermal degradation behaviour of pure PET, macadamia nut shell and its blend. A sample weight of ca. 0.700 g (±0.001 g) was used for each experiment. In the current study, five different sample compositions were used: pure PET (P_{100}) and pure macadamia nut shell (M_{100}), a blend of 80 wt.% of macadamia nut shell and 20 wt.% of PET ($M_{80}P_{20}$ blend), a blend of 50 wt.% of macadamia nut shell and 50 wt.% of PET ($M_{50}P_{50}$ blend), and a blend of 20 wt.% of macadamia nut shell – 80 wt.% of PET ($M_{20}P_{80}$ blend). All samples were heated in an alumina crucible under an atmosphere of flowing nitrogen up to 1480 K at heating rates of 3 °C/min, 5 °C/min and 8 °C/min. Low heating rates were chosen because they yield more reliable results [23]. The flow rate of purge gas was kept at 1 L/min. Weight changes were automatically measured and simultaneously recorded by computer.

2.3. Determining the kinetic parameters

Thermal degradation kinetics of PET, macadamia nut shell and their blends were evaluated by the Freeman–Carroll method. All kinetics studies refer to the following basic rate equation [24]:

$$\frac{d\alpha}{dt} = kf(\alpha) = k(1-\alpha)^n \tag{1}$$

where $f(\alpha)$ is the reaction model implying the actual reaction mechanism and k is the rate constant. According to Eq. (1), the rate of conversion at a constant temperature is a function of the reaction model and the rate constant. The conversion rate (α) can be calculated using the following equation:

$$\alpha = \frac{W_o - W_t}{W_o - W_f} \tag{2}$$

where W_o, W_f and W_t are the initial weight, the final weight and the weight at any time (t) respectively. The rate constant (k) is obtained by the Arrhenius equation:

$$k = A\ \exp^{-E_a/RT} \tag{3}$$

where A is the frequency factor, E_a is the apparent activation energy (kJ/mol), R is gas constant (8.314 J/mol), and T is the absolute temperature (K). Eq. (1) can be converted as follows:

$$\frac{d\alpha}{dt} = A\ \exp^{-E_a/RT} f(\alpha) = A(1-\alpha)^n \exp^{-E_a/RT} \tag{4}$$

$$\ln\frac{d\alpha}{dt} = \ln\ A + n\ln(1-\alpha) - \frac{E_a}{RT} \tag{5}$$

The following equations can be used to study the thermal degradation kinetics at a constant heating rate by converting Eq. (5) if small changes in temperature lead to negligible change in the apparent activation energy [25]:

$$\Delta\ln\frac{d\alpha}{dt} = n\Delta\ln(1-\alpha) - \frac{E_a}{R}\times\frac{1}{\Delta T} \tag{6}$$

This equation is known as Freeman and Carroll method and it describes the reaction rate $\frac{d\alpha}{dt}$ (%/min) for degradation reaction.

$$\frac{\Delta\ln(\frac{d\alpha}{dt})}{\Delta\ln(1-\alpha)} = n - \frac{E_a}{R}\times\frac{\Delta T^{-1}}{\Delta\ln(1-\alpha)} \tag{7}$$

If the differences in $\Delta\ln(\frac{d\alpha}{dt})$ and $\Delta\ln(1-\alpha)$ are obtained at regular intervals of $\frac{1}{T}$, the straight slope and intersect obtained from plot of $\frac{\Delta\ln(\frac{d\alpha}{dt})}{\Delta\ln(1-\alpha)}$ against $\frac{\Delta T^{-1}}{\Delta\ln(1-\alpha)}$ produces $\frac{-E_a}{R}$ and reaction order (n) respectively. The apparent activation energy and reaction order can be determined from the best-fit lines. Frequency factor (A) is then calculated using E_a and n in Eq. (5) [26–28].

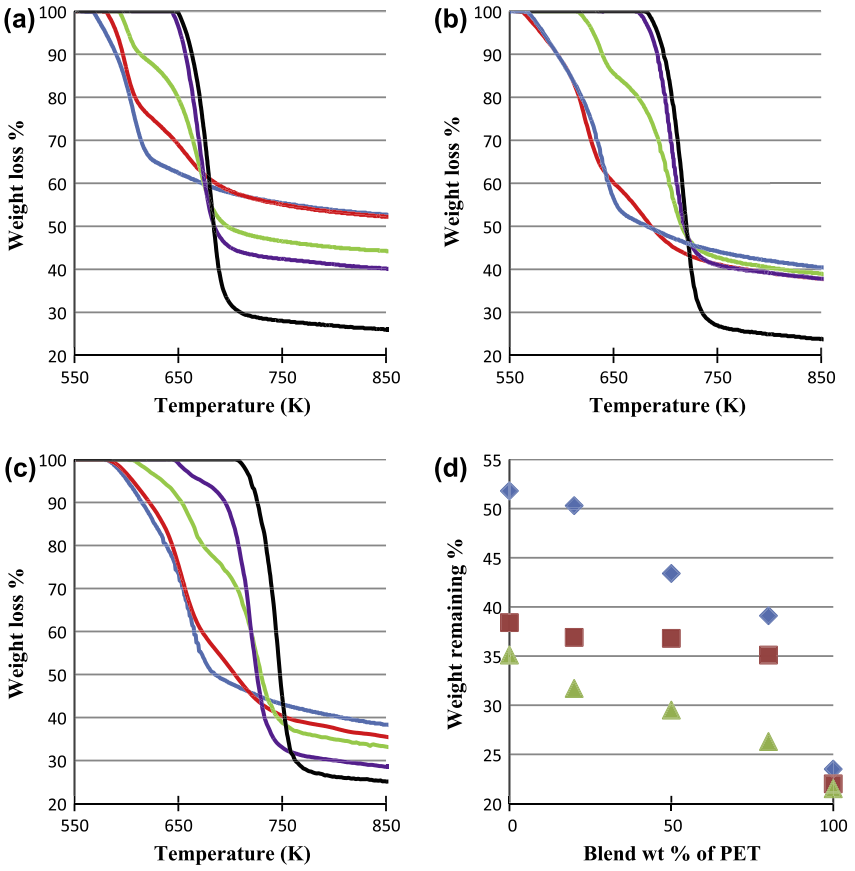

Fig. 1. TGA curves of samples heat treated at (a) 3 °C/min, (b) 5 °C/min, (c) 8 °C/min (— 100 wt.% macadamia nut shell, — 80/20 blends, — 50/50 blends — 20/80 blends, — 100 wt.% PET) and (d) final residue weight of blends heat treated at 3 °C/min (◆), 5 °C/min (■) and 8 °C/min (▲).

2.4. ^{13}C solid-state nuclear magnetic resonance (NMR) experiments

All NMR experiments were performed using BRUKER AVANCE III 300 spectrometer operating at ^{1}H NMR frequency of 300 MHz and ^{13}C NMR frequency of 75 MHz at room temperature. All samples were finely ground and ca. 75 mg were packed into 4 mm zirconia MAS rotor with kel-F $^{(R)}$ cap. A 4 mm double resonance MAS probehead was used to spin the sample to 8 kHz before recording the spectra. The sample groups heat treated at 5 °C/min analysed in NMR experiments can be divided into seven categories:

(a) Raw macadamia nut shell and raw PET.
(b) 100 wt.% Macadamia nut shell and PET pyrolysed up to 680 K
(c) Macadamia nut shell and PET separately pyrolysed up to 680 K and mixed in weight ratio of 80:20 ($M_{80}P_{20}$ mixture).
(d) Macadamia nut shell and PET blended together in an 80:20 weight ratio and then co-pyrolysed up to 680 K ($M_{80}P_{20}$ blend).
(e) Macadamia nut shell and PET single pyrolysed up to 730 K.
(f) Macadamia nut shell and PET separately pyrolysed up to 730 K and mixed in an 80:20 weight ratio ($M_{80}P_{20}$ mixture).
(g) Macadamia nut shell and PET blended together in an 80:20 weight ratio and then co-pyrolysed up to 730 K ($M_{80}P_{20}$ blend).

To obtain the ^{13}C NMR spectra, a ^{1}H–^{13}C cross-polarisation scheme with a 2 ms contact time with ramped polarisation transfer was used. The Total Suppression of Spinning Sidebands (TOSS) scheme [29] was used prior to detection to suppress overlap of the isotropic peaks with spinning sidebands.

3. Results and discussion

3.1. Thermal degradation behaviours of macadamia nut shell, PET and their blend

Fig. 1(a–c) shows the thermogravimetric (TG) curves of the pure and blended samples heat treated at 3, 5 and 8 °C/min. It can be seen that pure macadamia nut shell has the lowest thermal stability, degrading at 550 K, while pure PET degrades at a higher temperature 640 K. The TGA results indicate that increasing macadamia nut shell fraction in the blend increases the final residue weight. On the other hand, increasing the heating rate reduces the amount of final residue obtained from the pyrolysis. In particular as heating rate increases, the final residue weight of neat macadamia nut shell (M_{100}) rapidly decreases, while that of neat PET (P_{100}) remains relatively stable. This indicates that the thermal degradation behaviour of macadamia nut shell plays a primary role in determining the variation of the thermal degradation mechanism for the blend through a possible secondary reaction with the hydrocarbon volatiles from PET.

The final weight of residues for the different blend ratios and heating rates is shown in Fig. 1(d). The final residue weight is significantly affected by blending ratio and heating rate. As the weight fraction of PET in the blend or heating rate is increased, there is a reduction in the final residue weight. The least amount of char residue is obtained for the $M_{20}P_{80}$ blend heated at 8 °C/min while the $M_{80}P_{20}$ blend heated at 3 °C/min produces the highest char residue (51t wt.%) which comparable with that of M_{100} (52 wt.%). While it is expected that increasing macadamia nut shell content increases the char yield, the unique effect is that the char formation from the PET fraction also increases. In the specific case of the $M_{80}P_{20}$ blend

heated at 3 °C/min, if we assign 80% of the char weight to the macadamia fraction (i.e., 40.8 wt.%), we have a 10.8 wt.% contribution from the 20 wt.% PET fraction towards char formation. This implies that compared to neat PET where char yield is ca. 25 wt.%, char yield from the PET in the blend is nearly 50%. This increase in the char residue from the PET in the presence of the macadamia is indicative of a synergistic effect between the biomass and the PET. This effect is also seen in other blend concentrations and heating rates although to a lesser degree.

The origins of this synergistic effect can be more readily analysed by looking at the differential thermogravimetric (DTG) curves obtained from the TGA data. Fig. 2(a–c) shows the DTG curves for the neat and blended samples at heating rates of 3 °C/min, 5 °C/min and 8 °C/min respectively. The neat macadamia nut shell shows two main degradation regions from 550 K to 1075 K. Thermal degradation of hemicellulose corresponds to the shoulder in the DTG curve at ca. 550 K and takes place over a short temperature range, while the maximum loss peak of DTG curve at ca. 590 K accounts for the thermal degradation of the cellulose. The lignin degradation peaks appear as a tail section on the DTG curves at higher temperatures of ca. 1000 K [12,30,31]. In contrast to the neat macadamia nut shell, neat PET shows a single peak with maximum degradation rate at ca. 710 K which is higher than that of the macadamia nut shell. This is because the activation energy of the PET is relatively higher than that of macadamia nut shell [18]. A comparison of the DTG graphs at different heating rates shows that the temperature to initiate the degradation is shifted to higher temperatures with increasing heating rate due to the heat transfer effect at high mass loading [32–34]. The difference in the DTG curves for the different blend ratios indicates differences in the thermal degradation mechanisms. The DTG curves of the $M_{80}P_{20}$ and $M_{50}P_{50}$ blend show two maxima for at all heating rates. In contrast, there is only a single peak maxima occurring for $M_{20}P_{80}$ blend similar to the neat PET at heating rates of 3 °C/min and 5 °C/min. However 8 °C/min heating rate of the $M_{20}P_{80}$ blend shows a broad shoulder before the main peak indicating the occurrence of faster degradation.

3.2. Analysis of the synergistic effect during co-pyrolysis

The synergistic effect of reaction between macadamia nut shell and PET at a given temperature during co-pyrolysis can be characterised by the value of ΔM^T [35], defined as:

$$\Delta M^T = \text{weight loss}^T_{blend} - (\chi_1 \text{ weight loss}^T_1 + \chi_2 \text{ weight loss}^T_2) \quad (8)$$

where the weight loss^T_{blend}, weight loss^T_1 and weight loss^T_2 are weight losses of blend, macadamia nut shell and PET at instance time and at the same temperature, respectively. χ_1 and χ_2 are weight fraction of macadamia nut shell and PET in the blend. Therefore, ΔM^T is the extent of synergistic effect during co-pyrolysis. Increase in negative value of ΔM^T indicates higher synergistic effect of co-pyrolysis for the formation of char. ΔM^T monitors how effectively reactions occur between two materials compared with pyrolysis of single components, and then mixed at the same weight fraction as the co-pyrolysis blends.

Fig. 3 shows the plots of the synergistic effects (ΔM^T vs. T) along with the DTG curves of the co-pyrolysis ($d\alpha/dt$ vs. T) for $M_{80}M_{20}$, $M_{50}P_{50}$ and $M_{20}P_{80}$ blend samples, heat treated at 3 and 8 °C/min. The synergistic curves show two peaks (regions) that can be associated with a first and second synergistic effect respectively. The synergistic effect of the first peak (at the lower temperature) can be explained by the secondary reaction between hydrogen from PET and primary pyrolysis product of macadamia nut shell which is char. The second synergistic effect is permanent in the course of pyrolysis as seen by the negative value of ΔM^T all the way up

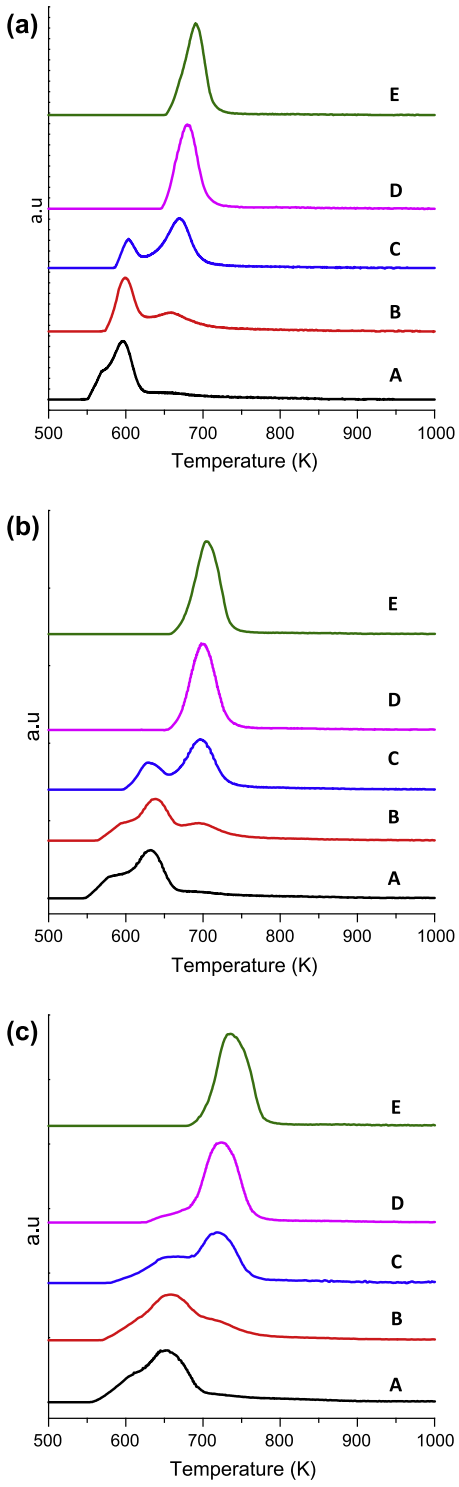

Fig. 2. DTG curves of samples heat treated at (a) 3 °C/min, (b) 5 °C/min and (c) 8 °C/min (A: 100 wt.% macadamia nut shell, B: $M_{80}P_{20}$ blends, C: $M_{50}P_{50}$ blends, D: $M_{20}P_{80}$ blends and E: 100 wt.% PET).

to the end of the reaction and it is accompanied by formation of thermally resistant carbon structure. The first synergistic effect for all the blends starts to occur at a temperature of ca. 570 K. Typically, biomass starts to form free radicals at 575 K and it is believed to be completely degraded by about 670 K, is a source of radicals [16,36]. It is important to know that the radical formation on char plays a key role in forming secondary char from organic vapours by catalysing the secondary reaction [14,30]. In

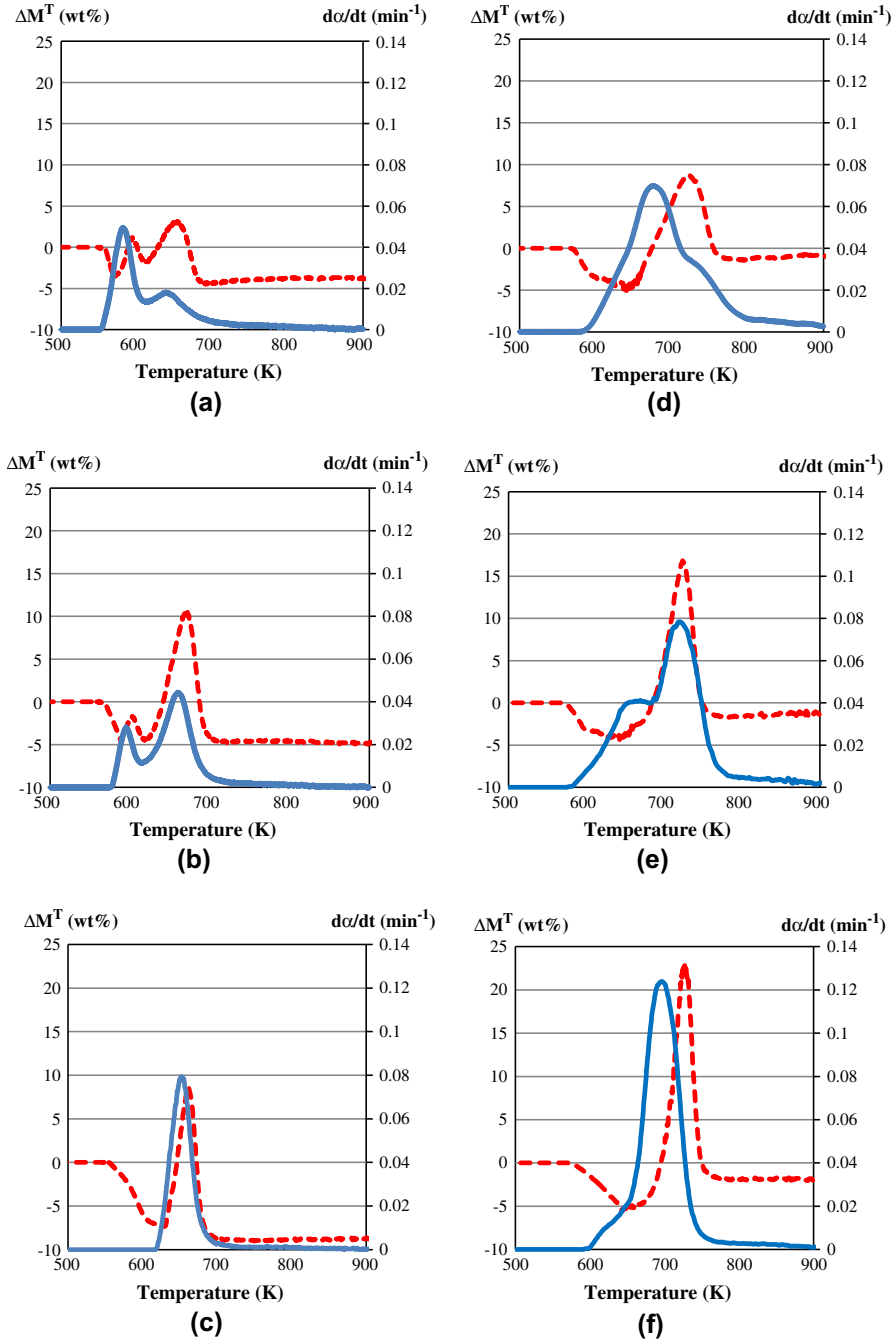

Fig. 3. (a) $M_{80}P_{20}$, (b) $M_{50}P_{50}$, (c) $M_{20}P_{80}$ heat treated at 3 °C/min, (d) $M_{80}P_{20}$, (e) $M_{50}P_{50}$ and (f) $M_{20}P_{80}$ heat treated at 8 °C/min (····· synergistic effect, —— DTG curve).

addition, PET begins to be thermally degraded at 670 K, and then simultaneous decrease in fluidity with production of a large amount of gaseous products between 670 K and 720 K [37,38]. Therefore the main degradation reaction zones of the two raw materials are partially overlapped. The radicals formed on macadamia nut shell cause the homolytic scission of the polyolefinic chains formed from PET degradation and causes hydrogen to be transferred from these chains to the radicals, thereby delaying the thermal degradation of macadamia nut shell in the low temperature region [16,39,40]. This hydrogen transfer which increases the macadamia nut shell's resistance to thermal degradation is the source the observed first-synergistic effect.

As degradation process proceeds further, the hydrogen transfer effect diminishes and the blend rapidly loses the first synergistic effect as indicated by an increase in the positive value of ΔM^T [17]. The second synergistic effect is initiated when the temperature reaches a critical point where PET degrades. PET degradation releases a variety of products such as CO, CO_2, methane, ethane, hydrogen, gases rich in PAHs compounds with oxygen functionalities, and oil with a scarce fraction of aliphatic hydrocarbon and large amount of aromatic hydrocarbons [41,42]. These products interact with the primary char from the macadamia nut shell and significantly contribute to the second synergistic effect which maximises the char residue upon completion of pyrolysis. The second synergistic effect is seen to be permanent for the PET–macadamia blend system, which is very different from other co-pyrolysis studies involving polymers such as HDPE, LDPE or PP and biomass [18,43], where the synergistic effect is not permanent. All blends

showed a higher second synergistic effect regardless of the heating rates. This implies that the char from the macadamia nut shell significantly contributes to the development of PAHs during co-pyrolysis.

3.3. Kinetic analysis of the thermal degradation

While the combination of the ΔM^T and DTG data gives us a qualitative understanding of the synergistic effects during co-pyrolysis, evaluating the kinetic parameters of the co-pyrolysis yields quantitative insights into the synergistic reactions between the blend components. A higher activation energy (E_a) and reaction order (n) for thermal degradation implies a greater thermal stability and a complex thermal degradation mechanism occurring in the solid state. The activation energy (E_a) yields a quantitative measure of the energy threshold for the formation of the product during pyrolysis. The reaction order (n) is an indication of the reaction mechanism for the thermal degradation while the frequency factor (A) is a measure of the frequency for molecules collisions regardless of the energy level during the reaction. In the case of pyrolysis, the E_a characterising the all the reaction processes which consisting of the breakdown of the organic molecules and evolution of new high molecular weight compounds during carbonisation. An increase in the reaction order (n) as the pyrolysis reaction progresses indicates a complex thermal degradation mechanism occurring in the solid state [25,27,44–46].

The DTG data from the M_{100} and P_{100} (data not shown) and the co-pyrolysed blend is analysed according to the Freeman–Carroll method and plotted in Figs. 4 and 5, which shows straight line graphs that have been fitted to yield the kinetic parameters E_a (the slope) and the reaction order n (the y-intercept). These kinetic parameters are listed in Tables 1–3 for the neat material and the blend samples. The M_{100} provides two sets of kinetic parameters associated with the two peak maxima seen in the DTG curves as seen in Table 1. As seen in Fig. 1(d), the weight of the char residue is inversely proportional to the heating rate. Concomitant to this observation, as the heating rate increases, the kinetic parameters E_a and n show a rapid decrease which is associated with the reduction in the residue weight. While the frequency factor (A) exhibits no temperature dependency, the frequency factor ($\ln A$) is seen to decrease with increase in the heating rate, which indicates a decrease in the molecular collision frequency with increasing heating rate. This decrease can be explained by the fact that the increased rate of energy input into the system causes a degradation of the material followed by rapid volatilization of the degradation products resulting in a decrease in the molecular collisions in the condensed reaction mixture. Therefore, the occurrence of simple reaction mechanism is expected as heating rate increases. As a result, an increase in heating rate significantly reduces char formation [46,47]. The hemicellulose and cellulose decomposition is a first order reaction while lignin decomposition is of a higher order. However simultaneous multi-component degradation of these three main components leads to a single nth – order reaction of value greater than one [46,48–51]. Thus the value of n yielded by the Freeman–Carroll analysis of the DTG data describes a pseudo-mechanism for the main component degradation as well as the secondary reaction leading to the char formation [15,52–54]. In the case of the secondary reaction, char formed during primary pyrolysis provides the organic tar with active sites to catalyse the conversion of the tar into secondary char. Hydrogen exchange reaction from the tar to the char is believed to increase the activation energy [55]. Therefore the reduction in the activation energy with increased heating rate would be consistent with a reduction in the hydrogen exchange reaction leading to reduction in char formation. Similarly n, which measures the formation of complex solid reaction products (char), also decreases with increasing heating rate. This effect is consistent with the reduced hydrogen transfer reactions (as measured by decrease in E_a) with the overall effect of reduced char formation. This observed effect is most prominent at lower temperatures (shoulder region in Table 1). The decreases in activation energy and reaction order represent faster thermal degradation and simpler reaction mechanism respectively. The decrease in the E_a and n with increased heating rates at higher temperatures (peak region in Table 1) is not significant as the shoulder region, which indicates that at the elevated temperatures the heat transfer rate no longer has a significant influence on the secondary char formation.

The neat PET (P_{100}) degradation on the other hand is much simpler as it consists of only one type of monomer and therefore the DTG shows a single peak at all heating rates. While PET degradation also showed a decrease in the activation energy with increasing heating rate (Table 2), the reaction order was more stable than that of the macadamia nut shell. The values for the kinetic parameter for PET degradation agree well with the results from previous studies [56–58], which indicates the uniformity of this material from different sources. The kinetic parameters of the macadamia nut shell degradation on the other hand are quite different for that reported for other biomass, which indicates that biomass from different sources can have very different degradation behaviour [53,59].

Considering the complexity of degradation kinetics for the neat materials, the reactions during co-pyrolysis are expected to be even more complex. In particular the change in the blend ratio is expected to have an impact on the kinetic parameters. The Freeman–Carroll analysis of the pyrolysis of the $M_{80}P_{20}$ and $M_{50}P_{50}$ blends yields two sets of kinetic parameters consistent with the two peak maxima observed in the DTG curves, while the $M_{20}P_{80}$ blend yields a single set of kinetics parameters for the lower heating rates. For the $M_{80}P_{20}$ and $M_{50}P_{50}$ blend, at the lower temperature regime (1st peak) the E_a increases with increasing PET fraction, as seen in Tables 3a–3c. This increase in the E_a can be assigned to the increased hydrogen transfer from the PET degradation products to the primary char. In fact the E_a of the first peak in the blend is higher than that of neat macadamia nut shell which is consistent with enhanced hydrogen transfer from the PET which is a stable source for the hydrogen at the elevated temperatures (unlike cellulose and hemicellulose which degrade below the temperatures of primary char formation). Crucially, along with the increase in E_a, an increase in the reaction order of the blend with increasing weight fraction of PET was also observed. In particular the $M_{50}P_{50}$ blend at all heating rates maximised reaction order during the first synergistic effect (1st peak in Tables 3a–3c). This indicates that the enhanced hydrogen transfer from the PET does indeed assist in stabilizing the primary product.

The extent of the radical effect on the thermal degradation of the PET is measured by the second activation energy and reaction order (2nd peak in Tables 3a–3c) and is associated with the second synergistic effect. According to kinetic data for second peak, the E_a has the following trend at all heating rates:

$$M_{20}P_{80}\text{ blend} > M_{50}P_{50}\text{ blend} > M_{80}P_{20}\text{ blend}$$

while the reaction order has the opposite trend:

$$M_{80}P_{20}\text{ blend} > M_{50}P_{50}\text{ blend} > M_{20}P_{80}\text{ blend}$$

As seen in Tables 3a–3c, the activation energies of PET in the blend are always lower than that of pure PET due to influence of the char which catalyses the PET degradation. This is in agreement with previous studies used other plastics and PET [39,40,60]. On the other hand, maximum reaction order for PET degradation is obtained from $M_{80}P_{20}$ blend which has the least amount of PET. This is due to the fact that the $M_{80}P_{20}$ blend has an excess of char from the macadamia nut shell which can more completely react

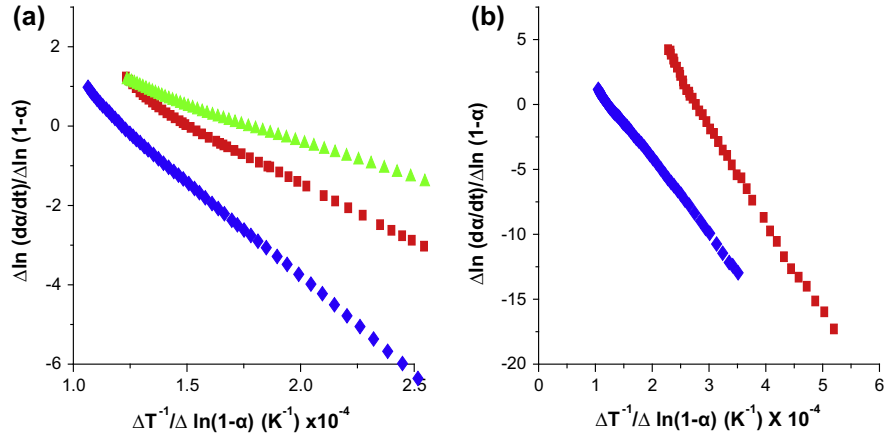

Fig. 4. (a) Variation of activation energy for first synergistic effect on $M_{80}P_{20}$ blends at different heating rates (◆ 3 °C/min, ■ 5 °C/min and ▲ 8 °C/min) and (b) variation of activation energy for first synergistic effect on blends at 3 °C/min (◆ $M_{80}P_{20}$ and ■ $M_{50}P_{50}$ blends).

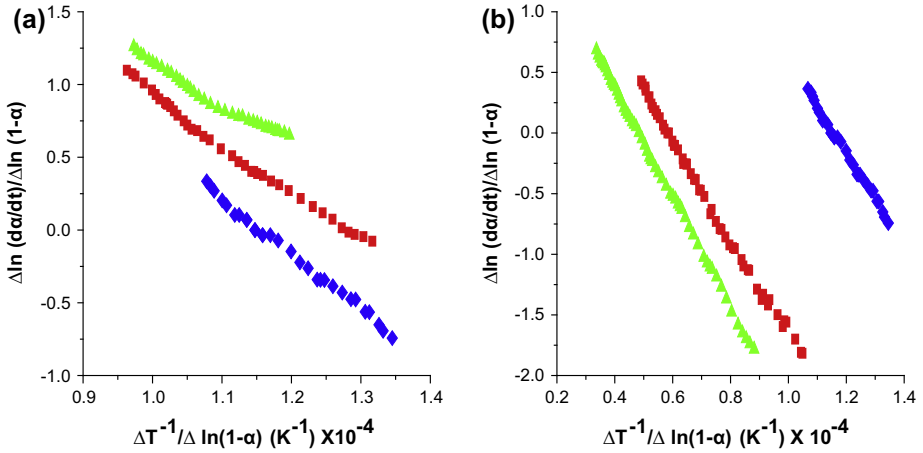

Fig. 5. (a) Variation of activation energy for PET degradation on $M_{80}P_{20}$ blends at different heating rates (◆ 3 °C/min, ■ 5 °C/min and ▲ 8 °C/min) and (b) variation of activation energy for PET degradation in blends at 3 °C/min (◆ $M_{80}P_{20}$, ■ $M_{50}P_{50}$ and ▲ $M_{20}P_{80}$ blends).

Table 1
Kinetic parameters for 100 wt.% of macadamia nut shell heat treated at 3, 5 and 8 °C/min.

100 wt.% Macadamia (°C/min)	E_a, kJ/mol		n		ln A, min^{-1}	
	Shoulder	Peak	Shoulder	Peak	Shoulder	Peak
3	334.0	286	10.1	3.2	64.9	54.4
5	188.7	206.2	9.7	3.0	36.0	38.0
8	129.4	132.9	4.8	2.5	22.7	24.7

Table 2
Kinetic parameters for 100 wt.% of PET heat treated at 3, 5 and 8 °C/min.

100 wt.% PET (°C/min)	E_a, kJ/mol	n	ln A, min^{-1}
3	331.6	1.8	56.1
5	283.3	1.9	46.7
8	198.2	1.9	34.5

with and capture the degradation products of the PET to yield higher concentrations of PAHs. At low macadamia nut shell concentrations such as in $M_{20}P_{80}$, while the char has catalysed the PET degradation, there is insufficient char to capture the PET products which are lost to volatilization. Thus it is important to vary the blend ratio yield the highest char production over the temperature range.

The thermal degradation of PET is known to follow a reaction order <2. However if a reaction order >2 is observed, it indicates the formation of thermally stable coke [61]. While the thermal degradation by second-order contributes to the weight loss of polymer by the intermolecular transfer and scission, the formation of polycyclic aromatic hydrocarbons (PAHs) is governed by a radical mechanism during which intermolecular and intramolecular aromatic condensation reactions occur. Thus increasing the amount of macadamia nut shell promotes both, the faster

Table 3a
Details of thermal degradation kinetics to samples heat treated at 3 °C/min.

3 °C/min	E_a, kJ/mol		n		ln A, min^{-1}	
	1st Peak	2nd Peak	1st Peak	2nd Peak	1st Peak	2nd Peak
$M_{80}P_{20}$	394.3 ± 22.5	269.2 ± 4.2	6.7 ± 0.2	4.2 ± 0.1	78.6 ± 4.2	47.0 ± 2.1
$M_{50}P_{50}$	545.8 ± 2.12	287.8 ± 9.4	20.5 ± 0.3	2.3 ± 0.1	104.4 ± 0.7	49.9 ± 1.1
$M_{20}P_{80}$	326.3 ± 15.6	2.0	55.9 ± 2.9			

Table 3b
Details of thermal degradation kinetics to samples heat treated at 5 °C/min.

5 °C/min	E_a, kJ/mol		n		ln A, min^{-1}	
	1st Peak	2nd Peak	1st Peak	2nd Peak	1st Peak	2nd Peak
$M_{80}P_{20}$	220.7 ± 2.9	204.7 ± 5.9	4.5 ± 0.1	3.9 ± 0.1	40.9 ± 1.7	40.3 ± 0.9
$M_{50}P_{50}$	299.5 ± 1.2	237.7 ± 4.2	12.6 ± 0.3	2.4	55.8 ± 1.9	39.9 ± 0.6
$M_{20}P_{80}$	277.1 ± 0.6		2.2		46.1	

Table 3c
Details of thermal degradation kinetics to samples heat treated at 8 °C/min.

8 °C/min	E_a, kJ/mol		n		ln A, min^{-1}	
	1st Peak	2nd Peak	1st Peak	2nd Peak	1st Peak	2nd Peak
$M_{80}P_{20}$	133.9 ± 3.0	155.6 ± 4.0	3.4 ± 0.1	3.2 ± 0.1	21.9 ± 1.2	28.5 ± 1.3
$M_{50}P_{50}$	147 ± 2.6	181 ± 15.4	6.4 ± 0.1	2.3	24.5	29.3 ± 2.9
$M_{20}P_{80}$	117.7 ± 5.5	190.7 ± 3.8	3.7 ± 0.1	2.0	27.4 ± 1.1	30.2 ± 0.4

degradation of PET and the formation of thermal stable structure by intensive cross-linking process. Therefore, in the $M_{80}P_{20}$ blend even though there is less PET-to-char hydrogen transfer at the lower temperature, at the higher temperatures where the PET degradation products are formed, the presence of the char maximises the aromatic condensation reaction which yields the maximum residue weight.

3.4. Nuclear magnetic resonance (NMR) study

The solid-state ^{13}C–^{1}H CPMAS NMR spectra (with Total Suppression of Spinning Sidebands) of macadamia nut shell and PET are shown in Fig. 6(a–f). The spectra show the difference in chemical complexities between the two materials as well as their degradation behaviour. The pyrolysis temperatures of 683 K and 734 K for the neat and blended materials were chosen to correspond to points before and after the DTG peak maxima which is related to the second synergistic effect. The complex spectrum of untreated macadamia nut shell (Fig. 6(a)) is very similar to previous studies of ligno-cellulosic materials [21,62–64]. This enables constituents within the matrix to be identified as follows: 104.5 ppm, 88 ppm, 72 ppm and 64 ppm for cellulose; 172 ppm, and 20.5 ppm for hemicellulose; 152 ppm, 148 ppm, 138 ppm, 113 ppm, 83 ppm, and 55 ppm for lignin. The detailed assignment of the peaks to specific chemical moieties has been previously presented by Melkior et al. [63]. Overall while the complex multi-component NMR spectrum of the neat macadamia nut shell mirrors the complex thermal degradation process observed, in contrast to the TGA method, NMR enables us to selectively monitor the pyrolytic degradation of the different components in the biomass.

The ^{13}C NMR spectrum of the as-received PET (Fig. 6(d)) is much simpler and has four peaks which correspond to the four unique carbon environments in the repeat unit of PET viz. 163 ppm for the ester carbonyl, 133.5 ppm for the unprotonated aromatic carbon, 130 ppm for the protonated aromatic carbon and 61.5 ppm for the alkoxy carbon [42,65]. Additionally PET is a semi-crystalline thermoplastic polymer and the amorphous domains are visible as broad shoulders at ca. 167 ppm and 64 ppm. Concomitant to its simple structure as seen in the ^{13}C NMR spectrum, the PET degradation is much simpler as compared to the macadamia nut shell.

The differences in the pyrolysis behaviour of the macadamia nut shell and the PET were also investigated with ^{13}C NMR spectroscopy. In particular we are able to monitor the changes in the chemical structure of the original materials as a function of heating temperature. ^{13}C NMR spectra of macadamia nut shell and PET heated to 683 K and 734 K are shown in Fig. 6. At 683 K, it is evident from the ^{13}C NMR that the macadamia nut shell has been significantly degraded. The predominant species remaining within the macadamia nut shell char are the aromatic carbons. The cellulose and hemicellulose are degraded completely and this is reflected by the complete absence of their correspond peaks in the ^{13}C NMR spectrum. In contrast however, some fragments of the lignin structure do survive at 683 K as is evidenced by the particularly characteristic lignin methoxy-peak at 55 ppm. Additionally new peaks appear in the alkyl region ca. 30–10 ppm which arise from the formation of low molecular weight tar from the breakdown of the cellulose and the hemicellulose. Additionally the formation of the dominant peaks at 126 ppm and 144 ppm in the aromatic region indicates the initiation of char formation consisting of aromatic ring structures originating from the lignin degradation and which will react with the tar residue to form secondary char [21,64] As the temperature of the pyrolysis is increased to 734 K, the degradation of the lignin component is accelerated and can be monitored by the significant reduction in the intensity of the methoxy peak at 55 ppm as seen in Fig. 6(c). At this temperature, a continued transformation of the aromatic carbon species to more fused ring type structures is also apparent from the reduction in the intensities of the phenolic species at 140–160 ppm as well as the reduction in the intensities of the aliphatic species between 30 and 10 ppm. However the fact the signal from the low molecular weight alkyl species has not disappeared completely implies that a mechanism of stabilization is at work which prevents their volatilization possibly. This stabilization effect may be assigned to the primary char physically trapping the low molecular weight components while catalysing their conversion to PAHs. This is consistent with the previous thermal degradation analysis of co-mixtures of cellulose and lignin [13].

In the case of PET, which is more thermally resistant to degradation than cellulose and hemicellulose, the ^{13}C spectrum of the sample treated at 683 K is very similar to the as received material (Fig. 6(d) and (e)). However the initiation of degradation at the less thermally stable ester carboxyl bond is visible by its reduced intensity in relation to the alkoxy or aromatic carbon species. Upon further temperature increase to 734 K, there is a rapid decrease in the intensities of ester carbonyl and alkoxy carbon signals. Another significant effect at this higher temperature is the complete breakdown of the crystalline domains and the formation of an essentially homogenous phase structure. This is seen by the disappearance of the sharp peaks and the appearance of much broader lineshapes in Fig. 6(f). Thus in the case of the PET, we are able to monitor both the chemical and phase transformations occurring during the pyrolysis.

Fig. 7(a) and (d) are spectra of macadamia nut shell and PET that were thermally treated separately and then mixed in an

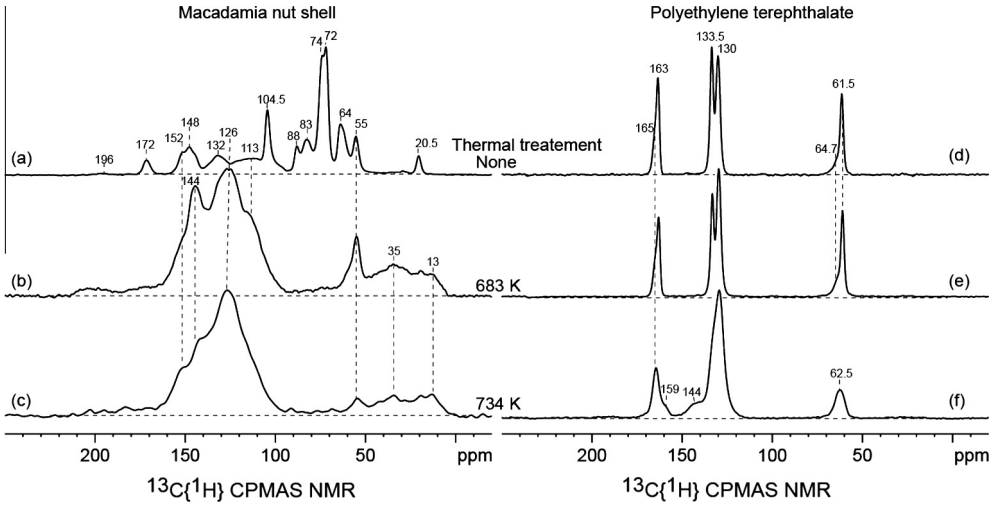

Fig. 6. $^{13}C\{^{1}H\}$-CPMAS NMR spectra of as received and pyrolysed macadamia nut shell (a–c) and as received and pyrolysed PET (d–f).

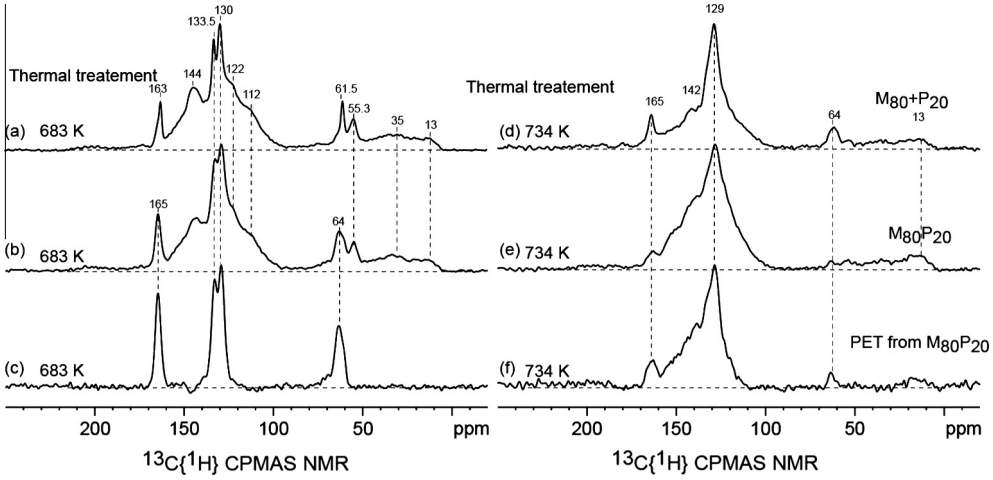

Fig. 7. $^{13}C\{^{1}H\}$ CPMAS with TOSS spectra of thermally treated 80 wt.% macadamia nut shell and 20 wt.% PET blend and mixture at 683 K (a–c) and 734 K (d–f) respectively. All spectra are scaled to the same intensity for clarity.

80–20 wt.% ratio ($M_{80} + P_{20}$ mixture). Fig. 7(b) and (e) are spectra of the neat macadamia nut shell and PET mixed in a 80–20 wt.% ratio ($M_{80}P_{20}$ blend) and then co-pyrolysed at 683 K and 734 K respectively. A comparison between the spectra in Fig 7(a) with (b) and Fig. 7(d) with (e) shows that there are distinct chemical and physical changes between the $M_{80} + P_{20}$ mixture and $M_{80}P_{20}$ blend at both 683 K and 734 K. The spectra in Fig 7(a) and (d) represent the case of no interaction between the Macadamia nut shell and PET during pyrolysis at either temperature. At 683 K, the signal from the PET in the mixture (Fig. 7(a)) shows well resolved peaks for the carbon sites (61.5 ppm, 130 ppm, 133.5 ppm and 163 ppm) which is identical to the signal in the neat PET (Fig. 6(e)), as expected. This comparison of the PET signal is similar for 734 K (compare Figs. 6(f) and 7(e)), where the PET peaks are similarly broadened due to the effect of the increased temperature. However in the case of the blend samples, the ^{13}C NMR signals of the PET look very different from the mixture, while the contribution to the ^{13}C NMR signal from macadamia nut shell does not show any marked difference. Thus we can subtract out the signal of the macadamia nut shell, to clearly visualize the difference in the PET. Fig 7(c) and (f) shows the signal of only the PET fraction within the heat treated $M_{80}P_{20}$ blend. The first evident result is the full conversion of the crystalline domains in the PET into an amorphous phase even at 683 K which is very distinct from the behaviour of neat heat treated PET. This is clearly demonstrated in Fig. 7(c), where the peak positions of the PET correlate to the peak positions of the amorphous component of the PET as seen in Fig. 6(d). We hypothesize that interaction with the hot volatiles formed during the degradation of the cellulose and hemicelluloses may be the cause for the early onset of phase change in the PET fraction of $M_{80}P_{20}$ blend. The spectra of the $M_{80}P_{20}$ co-pyrolysed at 734 K (Fig. 7(e)) shows a much more dramatic change in the structure of the PET as compared to the neat PET thermally treated to 734 K (Fig. 6(f)). In the case of the neat PET, there is an absence of any crystalline domains as well as the formation of two new ^{13}C NMR peaks at 144 ppm and 159 ppm (Fig. 6(f)). However the NMR signal from the PET domains in co-pyrolysed $M_{80}P_{20}$ (Fig. 7(f)) is very different where the major aromatic peaks are significantly broadened in comparison to the neat pyrolysed PET. Additionally there is signal intensity in the region between the ester group (165 ppm) and the primary aromatic peak (129 ppm). This indicates that there is a formation of complex disordered aromatic structures whose ^{13}C NMR signature is very similar to that of the aromatic species in the neat macadamia nutshell char (Fig. 6(c)). The ^{13}C NMR signal intensities at 160–140 ppm along with concomitant intensity at 120–110 ppm, indicates that there is

formation of phenolic species which is also an indication of char residue formation. Thus the spectrum in Fig. 7(f) clearly demonstrates the formation of char within the PET domains of the co-pyrolysed $M_{80}P_{20}$ mixture at 734 K unlike in the case of the neat PET. This result can be directly correlated to the occurrence of the PET degradation peak maxima at a lower temperature in the blend sample, as compared to the neat PET and it shows direct evidence that the presence of the macadamia does indeed promote char formation from the PET at reduced temperatures. Thus ^{13}C solid state NMR is able to characterise the distinct chemical and structural evolution which accompanies the synergistic effects and correlate this evolution to the measured reaction kinetics.

4. Conclusion

The synergistic effect for an increase in char formation by cross-linking reaction between macadamia nut shell and PET during co-pyrolysis has been confirmed by kinetic as well as chemical analysis by coupling the conventional TGA method with the ^{13}C solid state NMR technique. The synergistic effect is observed to increase the carbon yield from PET pyrolysis by a factor of two. The DTG data shows presence of two synergistic effects. The first effect is temporary and related to the hydrogen transfer to the primary char, while the second effect is permanent and related to the formation of PAHs from the PET. The Freeman–Carroll analysis of the DTG data shows that while the $M_{50}P_{50}$ blends yield the best kinetic parameters for char formation at lower temperatures (associated with the first synergistic effect), it is the $M_{80}P_{20}$ blend that yields the highest char residue due to more favourable kinetics at elevated temperatures (corresponding to the second synergistic effect). It is also shown by the analysis of kinetic parameters that increasing the heating rate has a negative impact on the first synergistic effect while the second synergistic effect is only marginally influenced. The chemical analysis of the solid residue of the best blend ratio ($M_{80}P_{20}$) by ^{13}C solid-state NMR shows that the crystalline domains in the PET transformed into an amorphous phase which is distinctly different from neat heat treated PET due to interaction with radicals. At higher temperature range (>690 K), extensive degradation of the PET in the blend and the formation of PAHs are detected. The correct assignment of the increased reaction orders, measured for the blend samples to the formation of condensed aromatic structures and PAHs is confirmed by their detection by solid-state NMR. The presence of aliphatic signals in the ^{13}C NMR indicates that the char from macadamia nutshell is able to capture volatiles from the PET, thereby enabling them to form char like structures. Thus the complex influence of reactant composition and heating rate on the product yield for pyrolytic processes can be comprehensively understood by the combination of kinetic analysis of the degradation process and the molecular-level understanding the reaction products. It is expected that such comprehensive analysis can enable the design of efficient pyrolysis conditions to maximise the yield high purity carbons from waste resources.

References

[1] Stephenson R. Macadamia: domestication and commercialization. Chron Horticult 2005;45(2):11–5.
[2] Shen L, Worrell E, Patel MK. Open-loop recycling: a LCA case study of PET bottle-to-fibre recycling. Resour Conserv Recycl 2010;55:34–52.
[3] Bockhorn H, Hentschel J, Hornung A, Hornung U. Environmental engineering: stepwise pyrolysis of plastic waste. Chem Eng Sci 1999;54:3043–51.
[4] Brebu M, Ucar S, Vasile C, Yanik J. Co-pyrolysis of pine cone with synthetic polymers. Fuel 2010;89:1911–8.
[5] Haque N, de Vries M. Greenhouse gas emission assessment of bio-coke from wood for application as bioanode in aluminium production. Proceedings of the 4th Annual high temperature processing symposium 2012, Melbourne, Victoria, Australia, 06–07 February 2012.
[6] Jung Y, Suh MC, Shim SC, Kwak J. Lithium insertion into disordered carbons prepared from organic polymers. J Electrochem Soc 1998;145:3123–9.
[7] Matthews M, Dresselhaus M, Endo M, Sasabe Y, Takahashi T, Takeuchi K. Characterization of polyparaphenylene (PPP)-based carbons. J Mater Res 1996;11:3099–109.
[8] Matthews M, Bi X, Dresselhaus M, Endo M, Takahashi T. Raman spectra of polyparaphenylene-based carbon prepared at low heat-treatment temperatures. Appl Phys Lett 1996;68:1078–80.
[9] Çit İ, Sınağ A, Yumak T, Uçar S, Mısırlıoğlu Z, Canel M. Comparative pyrolysis of polyolefins (PP and LDPE) and PET. Polym Bull 2010;64:817–34.
[10] Aydinli B, Caglar A. A degradation kinetic study on pyrolysis of three biomass samples and co-pyrolysis of hazelnut shell and ultra-high molecular weight polyethylene blends using a silver indicator. Energy Sources, Part A: Recovery, Utilization, Environ Eff 2013;35:900–8.
[11] Amen-Chen C, Pakdel H, Roy C. Production of monomeric phenols by thermochemical conversion of biomass: a review. Bioresour Technol 2001;79:277–99.
[12] Sannita E, Aliakbarian B, Casazza AA, Perego P, Busca G. Medium-temperature conversion of biomass and wastes into liquid products, a review. Renew Sustain Energy Rev 2012;16:6455–75.
[13] Sharma RK, Wooten JB, Baliga VL, Lin X, Geoffrey Chan W, Hajaligol MR, et al. Characterization of chars from pyrolysis of lignin. Fuel 2004;83:1469–82.
[14] Neves D, Thunman H, Matos A, Tarelho L, Gómez-Barea A. Characterization and prediction of biomass pyrolysis products. Prog Energy Combust Sci 2011;37:611–30.
[15] Di Blasi C. Modeling chemical and physical processes of wood and biomass pyrolysis. Prog Energy Combust Sci 2008;34:47–90.
[16] Marin N, Collura S, Sharypov VI, Beregovtsova NG, Baryshnikov SV, Kutnetzov BN, et al. Copyrolysis of wood biomass and synthetic polymers mixtures. Part II: characterisation of the liquid phases. J Anal Appl Pyrolysis 2002;65:41–55.
[17] Aboulkas A, El Harfi K, El Bouadili A. Non-isothermal kinetic studies on co-processing of olive residue and polypropylene. Energy Convers Manage 2008;49:3666–71.
[18] Zhou L, Wang Y, Huang Q, Cai J. Thermogravimetric characteristics and kinetic of plastic and biomass blends co-pyrolysis. Fuel Process Technol 2006;87:963–9.
[19] Kuznetsov B, Sharypov V, Kuznetsova S, Taraban'ko V, Ivanchenko N. The study of different methods of bio-liquids production from wood biomass and from biomass/polyolefine mixtures. Int J Hydrogen Energy 2009;34:7051–6.
[20] Woo Park J, Cheon Oh S, Pyeong Lee H, Taik Kim H, Ok Yoo K. A kinetic analysis of thermal degradation of polymers using a dynamic method. Polym Degrad Stab 2000;67:535–40.
[21] Freitas JCC, Bonagamba TJ, Emmerich FG. Investigation of biomass- and polymer-based carbon materials using ^{13}C high-resolution solid-state NMR. Carbon 2001;39:535–45.
[22] Keown DM, Li X, Hayashi J-I, Li C-Z. Characterization of the structural features of char from the pyrolysis of cane trash using Fourier transform-Raman spectroscopy. Energy Fuels 2007;21:1816–21.
[23] Wu H, Hanna MA, Jones DD. Thermogravimetric characterization of dairy manure as pyrolysis and combustion feedstocks. Waste Manage Res 2012.
[24] Vyazovkin S, Burnham AK, Criado JM, Pérez-Maqueda LA, Popescu C, Sbirrazzuoli N. ICTAC kinetics committee recommendations for performing kinetic computations on thermal analysis data. Thermochim Acta 2011;520:1–19.
[25] Ioannidou O, Zabaniotou A. Agricultural residues as precursors for activated carbon production—a review. Renew Sustain Energy Rev 2007;11:1966–2005.
[26] Paik P, Kar KK. Kinetics of thermal degradation and estimation of lifetime for polypropylene particles: effects of particle size. Polym Degrad Stab 2008;93:24–35.
[27] Farmahini-Farahani M, Jafari SH, Khonakdar HA, Böhme F, Yavari A, Tarameshlou M. Investigation of the thermal decomposition behavior and kinetic analysis of PTT/phenoxy blends. J Appl Polym Sci 2008;110:2924–31.
[28] Vuthaluru HB. Thermal behaviour of coal/biomass blends during co-pyrolysis. Fuel Process Technol 2004;85:141–55.
[29] Dixon WT, Schaefer J, Sefcik MD, Stejskal EO, McKay RA. Total suppression of sidebands in CPMAS C-13 NMR. J Magn Reson 1969;49(1982):341–5.
[30] Babu BV. Biomass pyrolysis: a state-of-the-art review. Biofuels, Bioprod Biorefin 2008;2:393–414.
[31] Tonbul Y. Pyrolysis of pistachio shell as a biomass. J Therm Anal Calorim 2008;91:641–7.
[32] Lin Y-C, Cho J, Tompsett GA, Westmoreland PR, Huber GW. Kinetics and mechanism of cellulose pyrolysis. J Phys Chem C 2009;113:20097–107.
[33] Becidan M, Skreiberg Ø, Hustad JE. Experimental study on pyrolysis of thermally thick biomass residues samples: intra-sample temperature distribution and effect of sample weight ("scaling effect"). Fuel 2007;86:2754–60.
[34] Skreiberg A, Skreiberg Ø, Sandquist J, Sørum L. TGA and macro-TGA characterisation of biomass fuels and fuel mixtures. Fuel 2011;90:2182–97.
[35] Cai J, Wang Y, Zhou L, Huang Q. Thermogravimetric analysis and kinetics of coal/plastic blends during co-pyrolysis in nitrogen atmosphere. Fuel Process Technol 2008;89:21–7.
[36] Balat M. Mechanisms of thermochemical biomass conversion processes. Part 1: reactions of pyrolysis. Energy Sources, Part A: Recovery, Utilization, Environ Eff 2008;30:620–35.
[37] Çit I, Sinag A, Tekes AT, Acar P, MisIrIloglu Z, Canel M. Effect of polymers on lignite pyrolysis. J Anal Appl Pyrolysis 2007;80:195–202.

[38] Vivero L, Barriocanal C, Álvarez R, Díez MA. Effects of plastic wastes on coal pyrolysis behaviour and the structure of semicokes. J Anal Appl Pyrolysis 2005;74:327–36.
[39] Aboulkas A, El harfi K, El bouadili A, Nadifiyine M, Benchanaa M, Mokhlisse A. Pyrolysis kinetics of olive residue/plastic mixtures by non-isothermal thermogravimetry. Fuel Process Technol 2009;90:722–8.
[40] Aboulkas A, El Harfi K, El Bouadili A. Pyrolysis of olive residue/low density polyethylene mixture: Part I thermogravimetric kinetics. J Fuel Chem Technol 2008;36:672–8.
[41] Brems A, Baeyens J, Vandecasteele C, Dewil R. Polymeric cracking of waste polyethylene terephthalate to chemicals and energy. J Air Waste Manage Assoc 2011;61:721–31.
[42] Suebsaeng T, Wilkie CA, Burger VT, Carter J, Brown CE. Solid products from thermal decomposition of polyethylene terephthalate: Investigation by CP/MAS ^{13}C-NMR and fourier transform-IR spectroscopy. J Polym Sci: Poly Chem Ed 1984;22:945–57.
[43] Chattopadhyay J, Kim C, Kim R, Pak D. Thermogravimetric characteristics and kinetic study of biomass co-pyrolysis with plastics. Korean J Chem Eng 2008;25:1047–53.
[44] Lapina NA, Ostrovskii VS, Syskov KI. Relationship between pyrolysis activation energy and graphitizability. Carbon 1976;14:39–41.
[45] Friedman HL. Kinetics of thermal degradation of char-forming plastics from thermogravimetry. Application to a phenolic plastic. J Polym Sci Part C: Polym Symp 1964;6:183–95.
[46] White JE, Catallo WJ, Legendre BL. Biomass pyrolysis kinetics: a comparative critical review with relevant agricultural residue case studies. J Anal Appl Pyrolysis 2011;91:1–33.
[47] Galwey AK, Brown ME. Application of the Arrhenius equation to solid state kinetics: can this be justified? Thermochim Acta 2002;386:91–8.
[48] Barneto AG, Carmona JA, Conesa Ferrer JA, Díaz Blanco MJ. Kinetic study on the thermal degradation of a biomass and its compost: composting effect on hydrogen production. Fuel 2010;89:462–73.
[49] Manyà JJ, Velo E, Puigjaner L. Kinetics of biomass pyrolysis: a reformulated three-parallel-reactions model. Ind Eng Chem Res 2002;42:434–41.
[50] Conesa JA, Domene A. Biomasses pyrolysis and combustion kinetics through n-th order parallel reactions. Thermochim Acta 2011;523:176–81.
[51] Caballero JA, Marcilla A, Conesa JA. Thermogravimetric analysis of olive stones with sulphuric acid treatment. J Anal Appl Pyrolysis 1997;44:75–88.
[52] Martín-Gullón I, Gómez-Rico MF, Fullana A, Font R. Interrelation between the kinetic constant and the reaction order in pyrolysis. J Anal Appl Pyrolysis 2003;68–69:645–55.
[53] Hashimoto K, Hasegawa I, Hayashi J, Mae K. Correlations of kinetic parameters in biomass pyrolysis with solid residue yield and lignin content. Fuel 2011;90:104–12.
[54] Hu S, Jess A, Xu M. Kinetic study of Chinese biomass slow pyrolysis: comparison of different kinetic models. Fuel 2007;86:2778–88.
[55] Mettler MS, Vlachos DG, Dauenhauer PJ. Top ten fundamental challenges of biomass pyrolysis for biofuels. Energy Environ Sci 2012.
[56] Encinar JM, González JF. Pyrolysis of synthetic polymers and plastic wastes. Kinetic study. Fuel Process Technol 2008;89:678–86.
[57] Saha B, Ghoshal AK. Thermal degradation kinetics of poly(ethylene terephthalate) from waste soft drinks bottles. Chem Eng J 2005;111:39–43.
[58] Cooney JD, Day M, Wiles DM. Thermal degradation of poly(ethylene terephthalate): a kinetic analysis of thermogravimetric data. J Appl Polym Sci 1983;28:2887–902.
[59] Caballero JA, Font R, Marcilla A. Comparative study of the pyrolysis of almond shells and their fractions, holocellulose and lignin. Product yields and kinetics. Thermochim Acta 1996;276:57–77.
[60] Aboulkas A, El Harfi K, El Bouadili A, Nadifiyine M. Study on the pyrolysis of Moroccan oil shale with poly (ethylene terephthalate). J Therm Anal Calorim 2010;100:323–30.
[61] Ohmukai Y, Hasegawa I, Mae K. Pyrolysis of the mixture of biomass and plastics in countercurrent flow reactor Part I: experimental analysis and modeling of kinetics. Fuel 2008;87:3105–11.
[62] Cheng HN, Wartelle LH, Klasson KT, Edwards JC. Solid-state NMR and ESR studies of activated carbons produced from pecan shells. Carbon 2010;48:2455–69.
[63] Melkior T, Jacob S, Gerbaud G, Hediger S, Le Pape L, Bonnefois L, et al. NMR analysis of the transformation of wood constituents by torrefaction. Fuel 2012;92:271–80.
[64] Bardet M, Hediger S, Gerbaud G, Gambarelli S, Jacquot JF, Foray MF, et al. Investigation with ^{13}C NMR, EPR and magnetic susceptibility measurements of char residues obtained by pyrolysis of biomass. Fuel 2007;86:1966–76.
[65] Maxwell AS, Ward IM, Lauprêtre F, Monnerie L. Secondary relaxation processes in polyethylene terephthalate-additive blends: 1. Nmr investigation. Polymer 1998;39:6835–49.